Supporting Information for

High temperature anionic Fe(III) spin crossover behavior in a mixed-valence Fe(II)/Fe(III) complex

Contents of the Supporting Information

Table S1. Crystallographic parameters for complexes **1** and **2**

Identification code	Complex_**1**	Complex_**2**
Empirical formula	$C_{46}H_{36}FeN_{12}O_6P$	$C_{184}H_{164}Fe_6N_{66}O_{29}$
Formula weight	939.69	4098.90
Temperature/K	100.01(10)	100.00(10)
Crystal system	triclinic	triclinic
Space group	$P\bar{1}$	$P\bar{1}$
a/Å	12.8708(3)	16.2038(4)
b/Å	13.1238(3)	16.8009(3)
c/Å	15.2393(4)	17.1213(3)
α/°	107.870(2)	82.518(2)
β/°	112.612(2)	74.902(2)
γ/°	100.095(2)	84.267(2)
Volume/Å^3	2131.90(10)	4451.26(16)
Z	2	1
ρ_{calc}g/cm^3	1.464	1.529
μ/mm^{-1}	3.747	4.603
F(000)	970.0	2118.0
2θ range for data collection/°	6.896 to 151.994	5.318 to 154.178
Reflections collected	19524	60753
Independent reflections	8336 [Rint = 0.0846, Rsigma = 0.0971]	18150 [Rint = 0.0428, Rsigma = 0.0437]
Data/restraints/parameters	8336/6/609	18150/6/1367
Goodness-of-fit on F^2	1.059	1.102
Final R indexes [I>=2σ (I)]	R1 = 0.0682, wR2 = 0.1600	R1 = 0.0498, wR2 = 0.1355
Final R indexes [all data]	R1 = 0.0927, wR2 = 0.1935	R1 = 0.0596, wR2 = 0.1412
Largest diff. peak/hole / e Å^{-3}	0.52/-0.54	0.99/-0.61

Table S2. Fe–O, Fe–N Bond lengths (Å) around Fe center and BVS values for Fe atom in complex **1**.

Complex 1		
Bond	**Bond Length / Å**	**Bond Valence**
Fe(1)–O(1)	1.894(3)	0.678
Fe(1)–O(3)	1.898(3)	0.670
Fe(1)–N(1)	1.926(4)	0.543
Fe(1)–N(6)	1.907(4)	0.571
Fe(1)–N(7)	1.911(4)	0.565
Fe(1)–N(12)	1.903(4)	0.578
	∑v(Fe) = 3.605	

Bond Valence = $\exp[(R_0-d_{ij})/b]$, R_0 = 1.70 for Fe(1)–N and 1.75 for Fe(1) –O, b = 0.37.[1]

Table S3. Fe–O, Fe–N Bond lengths (Å) around Fe centers and BVS values for Fe atoms in complex **2**.

Complex 2					
Bond	**Bond Length / Å**	**Bond Valence**	**Bond**	**Bond Length / Å**	**Bond Valence**
Fe(1)–O(1)	1.900(2)	0.667	Fe(2)–O(5)	1.890(2)	0.685
Fe(1)–O(3)	1.893(2)	0.679	Fe(2)–O(7)	1.889(2)	0.687
Fe(1)–N(1)	1.907(2)	0.572	Fe(2)–N(13)	1.921(2)	0.550
Fe(1)–N(6)	1.923(2)	0.547	Fe(2)–N(18)	1.935(2)	0.530
Fe(1)–N(7)	1.915(2)	0.559	Fe(2)–N(19)	1.923(2)	0.547
Fe(1)–N(12)	1.917(2)	0.556	Fe(2)–N(24)	1.925(2)	0.544
	∑v(Fe) = 3.580			∑v(Fe) = 3.543	

Bond	**Bond Length / Å**	**Bond Valence**
Fe(3)–N(25)	1.977(2)	0.333
Fe(3)–N(26)	1.984(2)	0.327
Fe(3)–N(27)	1.987(2)	0.324
Fe(3)–N(28)	1.990(2)	0.321
Fe(3)–N(29)	1.969(2)	0.340
Fe(3)–N(30)	1.969(2)	0.340
	∑v(Fe) = 1.985	

Bond Valence = $\exp[(R_0-d_{ij})/b]$, R_0 = 1.70 for Fe(1)/(2)–N, 1.75 for Fe(1)/(2)–O, 1.57 for Fe(3)–N, b = 0.37.[1]

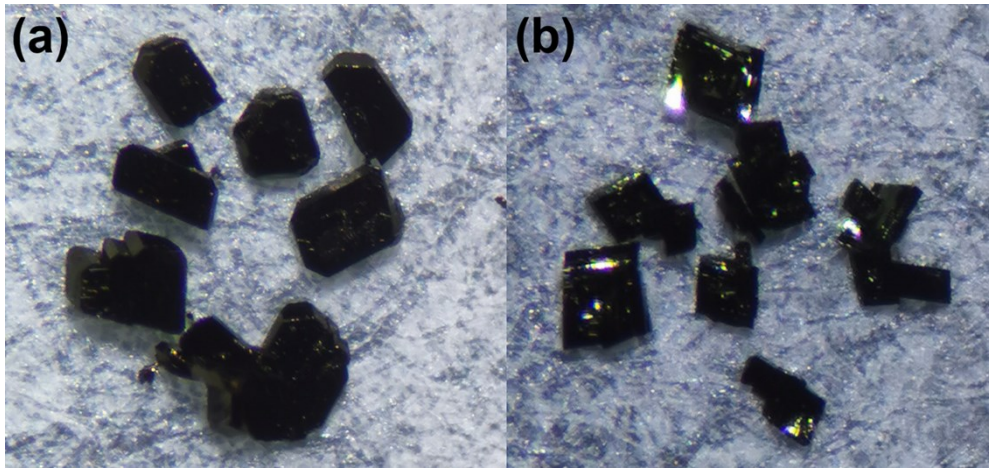

Fig. S1 Photographs of complexes **1** (a) and **2** (b).

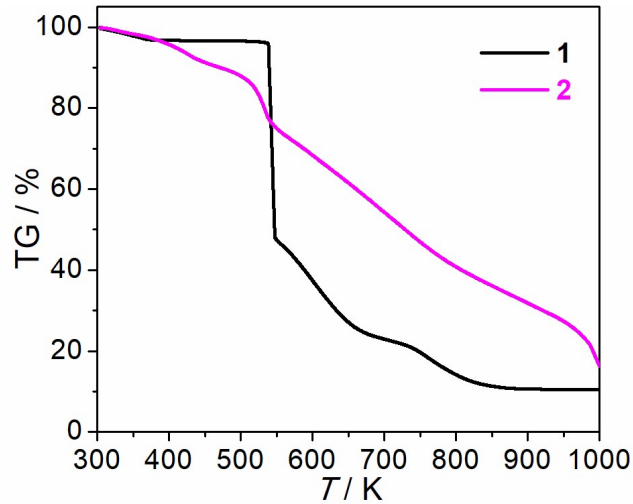

Fig. S2 TG curves of complexes **1** and **2**.

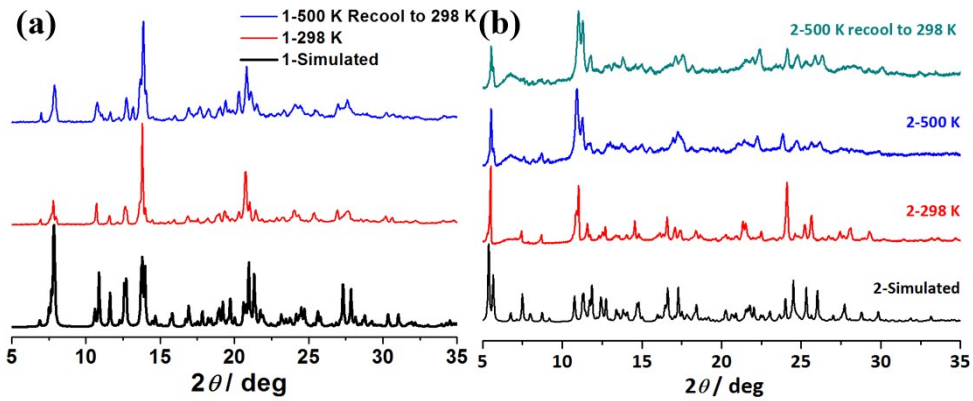

Fig. S3 PXRD patterns for simulations, 298 K and 500 K recool to 298 K of complexes **1** (a) and **2** (b).

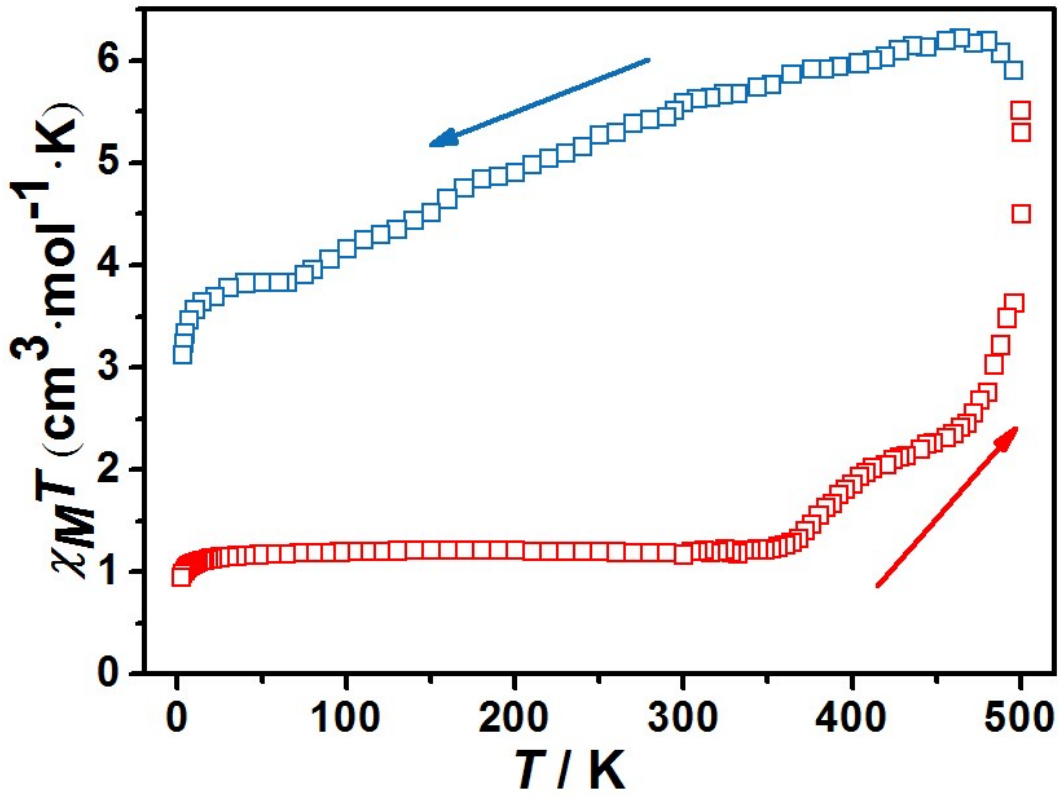

Fig. S4 Plot of χMT vs.T for complex **2**. The plot starts at 2 K, then the sample is warmed up to 500 K followed by cooling down to 2 K.

$\chi_M T$ of complex $[Fe^{II}(phen)_3][Fe^{III}(HATD)_2]_2 \cdot 3DMA \cdot 3.5H_2O$ **(2)** shows a value close to 1.2 $cm^3 \cdot K \cdot mol^{-1}$ from 10 to 360 K. Above this temperature, it increases abruptly to reach a value of 5.52 $cm^3 \cdot K \cdot mol^{-1}$ at 500 K, which corresponds to 50 % of the molecules in the HS state. When the sample is cooled from 500 to 60 k, this value decreases from 5.52 $cm^3 \cdot K \cdot mol^{-1}$ to 3.82 $cm^3 \cdot K \cdot mol^{-1}$. Below 50 K, the χMT decreases abruptly to reach a value of 2.50 $cm^3 \cdot K \cdot mol^{-1}$ at 2 K due to zero-field-splitting of HS Fe(III). This suggests that desolvation leads to irreversible structural changes that stabilize the HS state.[2]

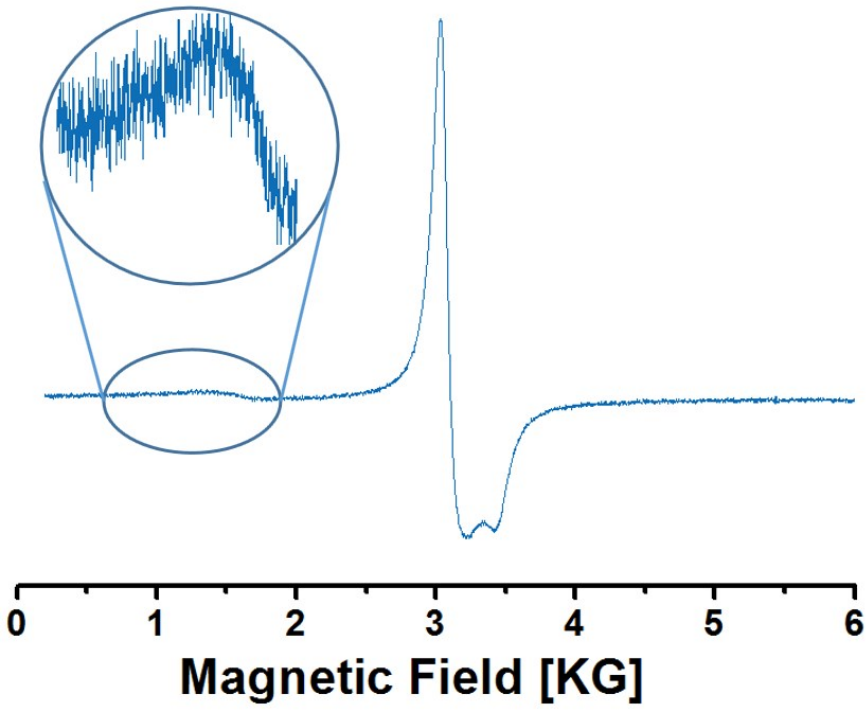

Fig. S5 EPR spectrum recorded at 500 K for complex **2** showing the trapped HS Fe(III) species (zoomedin portion of the spectrum).

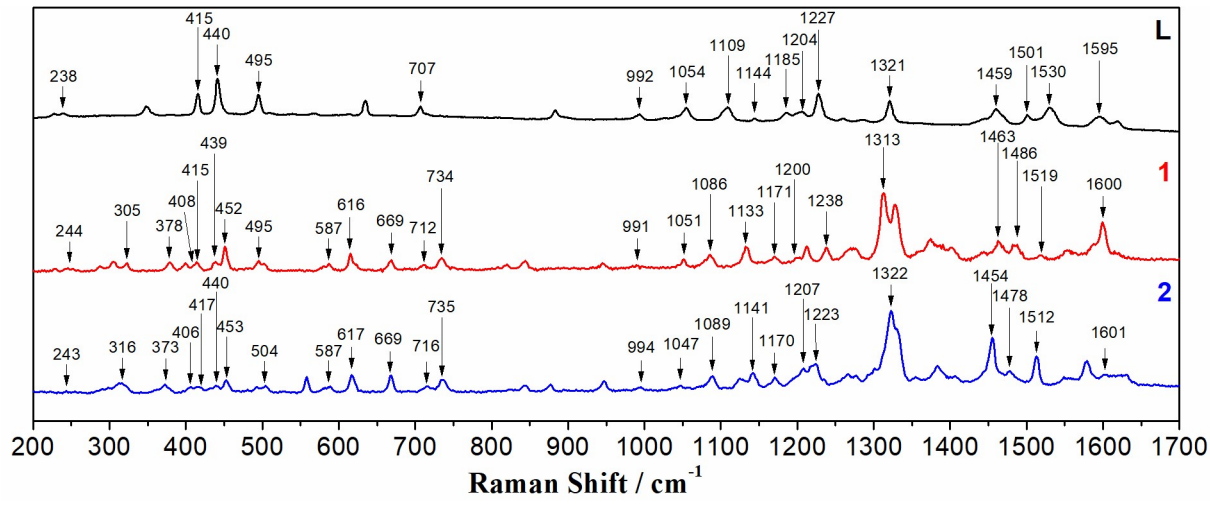

Fig. S6 Raman spectra for H_3ATD, **1** and **2** at room temperatures.

Table S4. Experimental Raman spectrum (cm^{-1}) for H_3ATD, **1** and **2** at room temperatures.

cm^{-1}			Assignments[2-6]
Ligand	**1**	**2**	
238	244	243	C=C bending (naph)
	322	316	Fe-O bending
	378	373	Fe-N bending
	408	406	Fe-O + Fe-N bending
415	415	417	C=C-N bending
440	439	440	O-C + N=N bending
	452	453	Fe-N bending
495	495	504	C=C bending (naph)
	587	587	Fe-N symmetric stretching
	616	617	Fe-N asymmetric stretching
	669	669	Fe-O symmetric stretching
707	712	716	C=C bending (naph)
	734	735	Fe-O bending
992	991	994	N=N bending
1054	1051	1047	C-H bending and stretching
1109	1086	1089	symmetric stretching (naph ring)
1144	1133	1141	C-H bending
1185	1171	1170	C-H bending + N-C stretching
1204	1200	1207	C-H bending + N-C stretching + C=C stretching (naph)
1227	1238	1223	C-H + N-C stretching
1321	1313	1322	symmetric stretching (tetrazole ring)
1459	1463	1454	symmetric stretching (tetrazole ring)
1501	1486	1478	symmetric stretch (naph ring)
1530	1519	1512	symmetric stretch (naph ring)
1595	1600	1601	C-H bending + symmetric stretch (naph ring) + N=N/C-N symmetric stretching

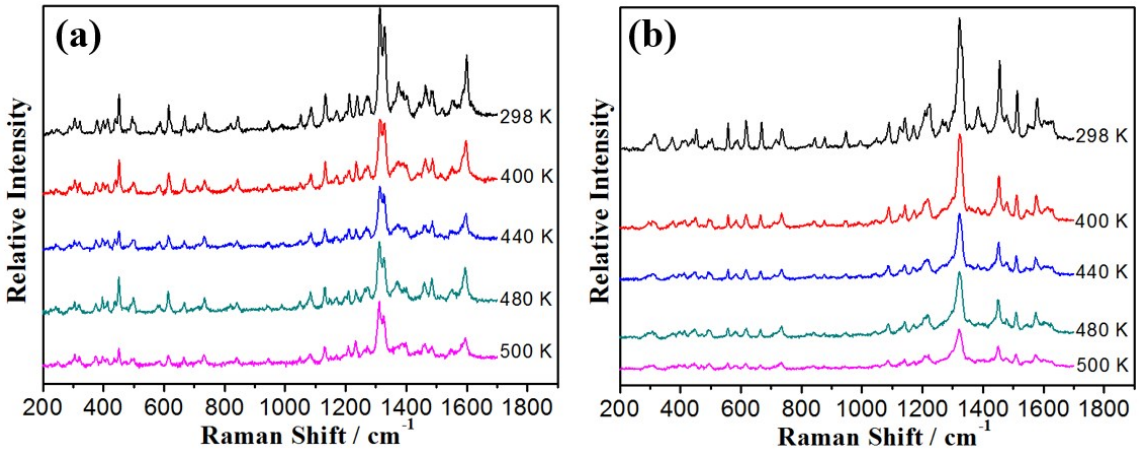

Fig. S7. variable-temperature Raman spectra of complexes **1** (a) and **2** (b) at 298 K, 400 K, 440K, 480 K, 500 K.

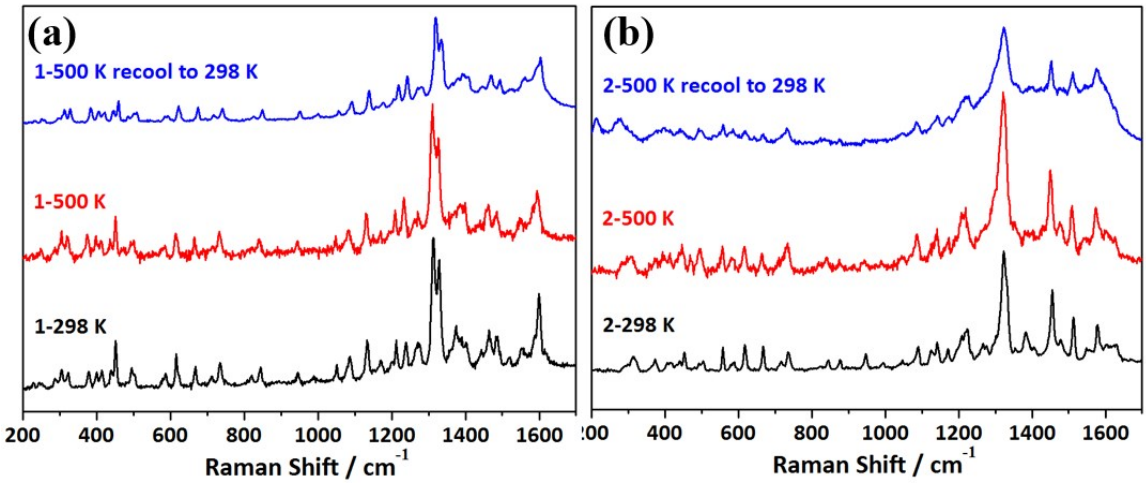

Fig. S8 Raman spectra for 298 K, 500 K and 500 K recool to 298 K of complexes **1** (a) and **2** (b).

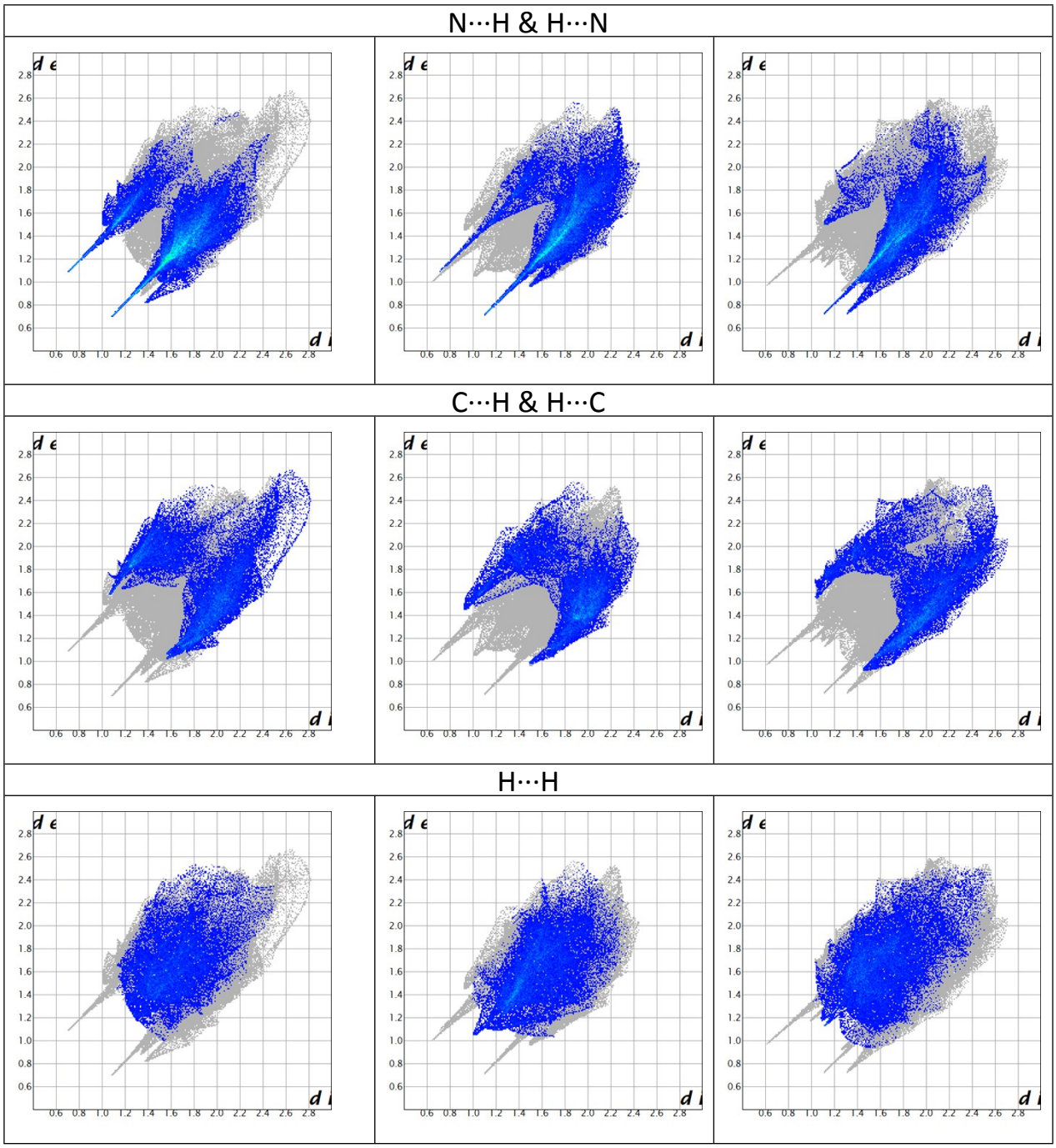

Fig. S9 N···H & H···N, C···H & H···C and H···H contact-decomposed 2D Fingerprint plots fo **1-Fe** (left column, **2-Fe-1** (bottom column) and **2-Fe-2** (right column). Grey zones represent all of the interactions and the blue zones account for the corresponding selected interactions.

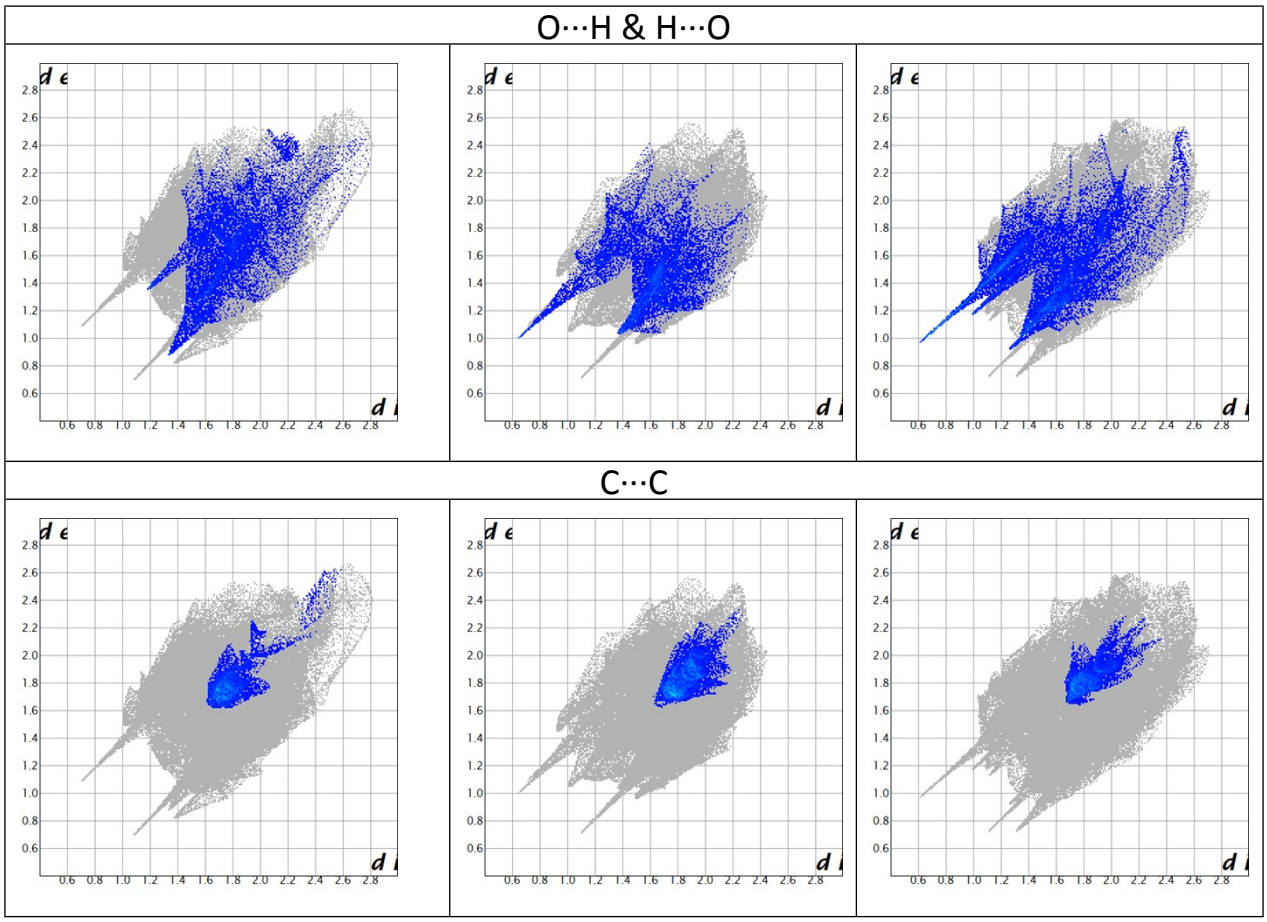

Fig. S10 O···H & H···O and C····C contact-decomposed 2D Fingerprint plots fo **1-Fe** (left column, **2-Fe-1** (bottom column) and **2-Fe-2** (right column). Grey zones represent all of the interactions and the blue zones account for the corresponding selected interactions.

References

1 H. Zheng, K. M. Langner, G. P. Shields, J. Hou, M. Kowiel, F. H. Allen, G. Murshudov and W. Minor, *Acta Crystallogr D Struct Biol*, 2017, **73**, 316-325.

2. A. J. Kunov-Kruse, S. B. Kristensen, C. Liu and R. W. Berg, *J. Raman Spectrosc.*, 2011, **42**, 1470–1478.

3. S. Ossinger, H. Naggert, E. Bill, C. Näther, and F. Tuczek, Inorg. Chem. 2019, 58, 12873−12887.

4. J. Bautz, P. Comba, and L. Q. Jr. *Inorg. Chem.*, 2006, **45**, 7077-7082.

5. Priyanka Gautam, Om Prakash, R.K. Dani, M.K. Bharty, N.K. Singh, Ranjan K. Singh, *J. Mol. Struct.*, 2017, **1127**, 489-497.

6. R. Meier, J. Maigut, B. Kallies, N. Lehnert, F. Paulat, F. W. Heinemann, G. Zahn, M. P. Feth, H. Krautscheid and R. V. Eldik, *Chem. Commun.*, 2007, 3960–3962.